Geomorphology 105 (2009) 171–181

Contents lists available at ScienceDirect

Geomorphology

journal homepage: www.elsevier.com/locate/geomorph

# Longitudinal ridges in mass movement deposits

A. Dufresne *, T.R. Davies

*Department of Geological Sciences, Canterbury University, Christchurch, New Zealand*

ARTICLE INFO

*Article history:*
Received 16 May 2008
Received in revised form 15 September 2008
Accepted 16 September 2008
Available online 26 September 2008

*Keywords:*
Rock avalanche
Longitudinal ridge
Flowbands
Mass movement
Granular flow

ABSTRACT

Prominent longitudinal features are often reported on the surfaces of mass movement deposits. However, the genesis and implications of these have not hitherto been considered, and herein we present preliminary observations of their occurrence both in the field and in the laboratory. Elongated ridges are often oriented (sub-) parallel to the flow direction and aligned radially from the source due to debris spreading. They are particularly prominent in large ($> 10^6 m^3$) rock avalanches emplaced onto deformable substrates and are also found in the proximal reaches of volcanic debris avalanches. Flowbands, which are longer and thinner expressions of longitudinal ridges, are continuous along the entire flow length and are observed in rock avalanches emplaced onto glaciers, in snow and some ice avalanches, in pyroclastic flows and some block-and-ash flows, in ejecta sheets, in extraterrestrial landslides, and in some volcanic debris avalanches. Other volcanic debris avalanches and the distal areas of rock avalanches often display hummocks that are aligned radially from the source; we propose that these aligned hummocks are remnants of longitudinal ridges. The formation of elongate ridges (and their expressions as flowbands, aligned hummocks, or distal lobes and digits) in qualitatively-similar fashion in both laboratory and field environments suggests they represent an intrinsic tendency of granular flows in a wide range of situations.



## 1. Introduction

Mass movements occur in a variety of geological materials (rocks, sediments, snow, ice), on different scales (large, $> 10^6 m^3$, rock and debris avalanches, smaller snow avalanches, sand on dunes, etc), and are found in almost any environment where slopes are present. They can also be produced in the laboratory where the small-scale flows mimic features and behaviours of their field-scale counterparts, providing conceptual models of feature formation and the opportunity to observe flow dynamics up close; however, careful attention to scaling is required.

A lively and continuing discussion in the literature on emplacement mechanisms and dynamics of rock and debris avalanches, pyroclastic and block-and-ash flows, and snow avalanches offers a wide range of models to explain runout, modes of emplacement and deposit characteristics of mass movements. Clearly the basic mechanism of mass movements is that of granular flow, even where large intact blocks (e.g. toreva blocks) are involved.

Herein we focus attention on one prominent and consistent morphological characteristic of the different types of mass movements and granular flows: that of more or less prominent ridging in the flow-parallel direction ("longitudinal ridging") observed on the surfaces of many avalanche deposits (see case studies below). We believe that this reflects processes active during the flow, as well as at the moment the flow comes to rest, and that it may therefore be used to infer aspects of flow dynamics. We offer suggestions on the formation of longitudinal ridges with respect to material properties, emplacement dynamics, and environmental factors such as topography and substrates. While we focus particularly on the occurrence and origin of longitudinal ridges, we also relate them to the occurrence of transverse ridges and hummocks. We begin with a definition of the features observed in the field, and with brief summary of granular flows and the basic processes of longitudinal ridging.

## 2. Longitudinal ridges and flowbands: definitions

Following the way the terms are generally used in the geological literature (for examples see list of references in Table 1) we offer the following general definitions.

Ridges stand prominently above the rest of the deposit by up to tens of metres and are usually found within the proximal to medial reaches of rock and debris avalanches. Smaller ridges are sometimes found at the distal margins where they grade into frontal lobes. Ridge lengths are typically on the order of hundreds of metres. The terms "ridge" and "elongate ridge" are often used interchangeably. However, the latter is preferentially applied as an emphasis when ridges are especially long, appearing stretched or extended (though no consistent threshold can yet be determined to precisely mark the difference) and/or when such long ridges are aligned parallel to the spreading direction.

Flowbands on the other hand do not stand out high above the rest of the deposit, are usually separated from adjacent parallel bands by

* Corresponding author. Tel.: +64 3364 2987; fax +64 3364 2769.
*E-mail address:* volcanja@web.de (A. Dufresne).

0169-555X/$ – see front matter © 2008 Elsevier B.V. All rights reserved.
doi:10.1016/j.geomorph.2008.09.009

**Table 1**
Data for hummock, ridge and flowband dimensions

| Deposit | Hummock | Ridge | Flowband | *L* [m] | *W* [m] | *H* [m] | *L*/*W* | *L*/*H* | *H*/*W* | Comments |
|---|---|---|---|---|---|---|---|---|---|---|
| Jocotitlan | x | | | 405 | 330 | 95 | 1.2 | 4.3 | 0.29 | Data from topographic map (arcview) using closed contours as base of hummock |
| | x | | | 443 | 347 | 105 | 1.3 | 4.2 | 0.30 | |
| | x | | | 215 | 180 | 45 | 1.2 | 4.8 | 0.25 | |
| | x | | | 455 | 328 | 115 | 1.4 | 4.0 | 0.35 | |
| Round top | x | x | | 100 | 95 | 17 | 1.1 | 5.9 | 0.18 | Height data estimates from field photos. *L* and *W* from morphological map. |
| | | x | | 200 | 95 | 17 | 2.1 | 11.8 | 0.18 | |
| | | x | | 380 | 120 | 12 | 3.2 | 31.7 | 0.10 | |
| | | x | | 350 | 110 | | 3.2 | | | |
| | | x | | 190 | 80 | | 2.4 | | | |
| Parinacota | x | | | | | | | 4 to 20 | | From Clavero et al. (2002); *L* is the average hummock diameter |
| Altenau | | x | | 377 | 100 | | 3.8 | | | Data extracted from geological map in von Poschinger (1994) |
| | | x | | 267 | 100 | | 2.7 | | | |
| | | x | | 233 | 78 | | 3.0 | | | |
| Lastarria | | | x | 2850 | 145 | 10 | 19.7 | 285.0 | 0.07 | *H* here is the average deposit thickness estimated; *L* is estimated from photo in Naranjo and Francis (1987) |
| Shasta | x | | | 800 | 630 | 146 | 1.3 | 5.5 | 0.23 | Data extracted from topographic map in Crandell et al. (1984) |
| | x | | | 567 | 400 | 73 | 1.4 | 7.8 | 0.18 | |
| | | x | | 2467 | 800 | 146 | 3.1 | 16.9 | 0.18 | |
| | x | x | | 1160 | 800 | 146 | 1.5 | 7.9 | 0.18 | |
| | x | | | 600 | 500 | 73 | 1.2 | 8.2 | 0.15 | |
| | | x | | 1930 | 330 | 85 | 5.8 | 22.7 | 0.26 | |
| Mombacho | x | | | 90 | 48 | 9 | 1.9 | 10.0 | 0.19 | Using averaged graph equations and highest occurrence hummock *L* and Shea et al. (2008) |
| Sherma glacier | | | x | 260 | 12 | 3 | 21.7 | 86.7 | | *L* and *W* estimated from high-resolution aerial photographs; *H* here is the average deposit thickness (McSaveney, 1978) |
| | | | x | 382 | 16 | 3 | 23.9 | 127.3 | | |
| | | | x | 165 | 6 | 3 | 27.5 | 5.0 | | |
| | | | x | 412 | 24 | 3 | 17.2 | 137.3 | | |

*L* = length, *W* = width, *H* = height of the respective features.

narrow "furrows", and generally extend along almost the entire flow length and hence can reach some kilometres in length. Flowbands can split into multiple bands, and in distal reaches they often form digits that sometimes curve in their paths and override other digits obliquely. Flowbands are also sometimes referred to as "striations" because deposits with narrow flowbands often look striated on aerial photographs (e.g. Shiveluch, Belousov et al., 1999; Fig. 5B). Another variety is a "herringbone" structure on individual flowbands. In this case, the flowbands exhibit V-shaped ridges pointing uphill as described by Naranjo and Francis (1987). These authors used the term "herringbone" to describe the features of the Lastarria debris avalanche deposit (see below and Fig. 5C) in accordance to its resemblance of structures observed in ejecta sheets found around impact craters, where the term was apparently coined.

A continuum of morphologies is apparent from hummocks, through ridges to flowbands. Hummocks have length-to-height (*L*/*H*) ratios generally less than ~ 10 (Fig. 1; some field examples are listed in Table 1) and length-to-width (*L*/*W*) ratios of ~ 1–2. These ratios increase to the 100s (*L*/*H*) and over ~ 20 (*L*/*W*) for flowbands. Values for ridges lie between the two. These rough definitions are based on available data from the literature and on our own field observations.

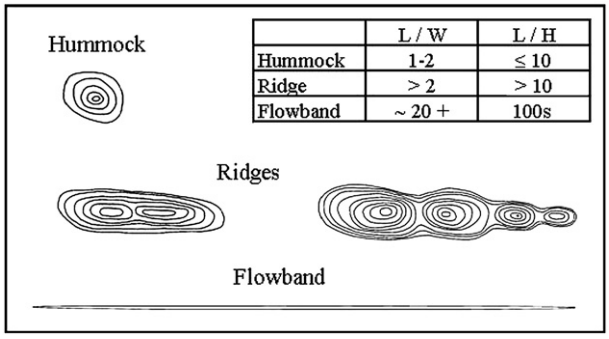


**Fig. 1.** Map-view of hummock, ridge and flowband geometries. Table insert shows the range of values of geometric relationships distilled from descriptions, maps and data presented in the literature.

## 3. Granular flow — basics and models

Herein we briefly summarise current knowledge of granular flow processes, and outline some published experimental results that suggest that longitudinal striations result from the physics of granular flow, rather than from large-scale environmental peculiarities of debris avalanches alone.

Granular flow is the gravity-driven motion of assemblages of individual solid grains during which the grains interact with each other and with the flow boundaries. Dry granular flow of noncomminuting, noncohesive grains over a rigid base is affected by only two external forces: gravity acting on each grain and friction from the base acting on the basal grains. The intergranular forces are complex; in general they can be anisotropic and heterogeneous. In particular, relative grain motion can be concentrated in narrow layers called "shear bands" (Francois et al., 2002); and shear forces are transmitted across shear bands by quasilinear assemblages of grains in compression, which are called "grain bridges" or "force chains" (Anthony and Marone, 2005); Fig. 2.

When a grain mass is saturated by water, additional forces arise from pore water pressure distribution and water motion; and the situation becomes still more complex — additionally so if part of the grain mass is unsaturated. Further complications arise when the grains themselves are of a range of sizes and shapes. At present, predicting the three-dimensional flow behaviour of variably sized, shaped, and saturated grain flows is not possible without substantial empirical input. Hence, although simple in concept, real-life grain flows are complicated in practice. In this context, the appearance of large-scale flow structures (such as ridges in a grain flow) is not a surprise, any more than the appearance of meanders in a river flow is a surprise; neither is predictable from the detail of the preceding steady uniform flow, but both emerge from the smaller-scale dynamics of the "simple" flow of water or grains.

The fact that longitudinal ridging has been reported in very simple and well-constrained laboratory situations (Pouliquen et al., 1997) indicates that this process is a very fundamental phenomenon of granular flow, and is therefore to be expected in more complex grain flows such as field-scale mass movements. In particular, Pouliquen et al. (1997) concluded that the initial instability is related to lateral

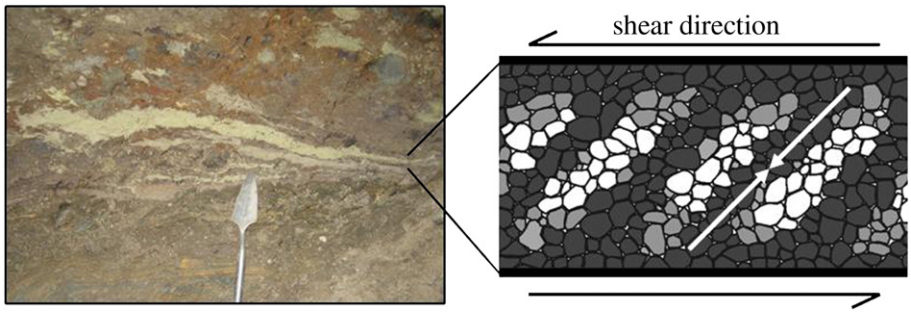


**Fig. 2.** Field example of shear bands preserved at the base of the Cantal rock avalanche deposit, France (20cm long tool for scale). The sketch to the right illustrates force distribution along grain bridges (arrows) in a granular mass experiencing shear: dark grains within the grain bridges are under higher stresses than the lighter coloured ones.

segregation of grains of different sizes at the front of the flow, because with uniformly sized spherical glass beads they observed no ridging. They introduced larger grains in the form of crushed fruit stones or coarse, irregular beads to generate ridging, which suggests that grain shape and/or density may also have played a role. In a later experiment, Pouliquen and Vallance (1999) found no ridging-type instability in dry flows with mixtures of coarse and fine glass spheres, or in any saturated flows; this suggests that the coarse grains must be angular and that the flow must be less than fully saturated to cause prominent ridging.

All the above experiments took place on rough rigid beds. By contrast, Aranson et al. (2006) studied the theoretical stability of granular avalanches on an erodible bed, using a continuum approach with no grain size specified. They found that lateral instability, which further develops into ridging as a causative factor in the ridging process, occurred if the static and dynamic friction coefficients differed, which is the case for all granular flows, but particularly so for a mixture of small spherical and large angular grains. They also found that ridging would occur under water, with saturated flows. Mallogi et al. (2008) confirmed these results experimentally; in particular, they found that transverse instability occurred whenever the angle of inclination of the substrate was greater than some critical value, and ridging developed as a result of coarsening, although their granular material was narrowly graded. The existence of a threshold angle for transverse instability may suggest that relatively high-velocity flows are more liable to ridging.

In our own experiments a small volume (200ml) of sand was dropped through a 100-cm-long tube onto a metal runout surface, 30cm wide, just above the slope transition from 60° to 0° inclination (Fig. 3A). The sand avalanche developed flow front irregularities in the form of small undulations (Fig. 3B), which, however, were short-lived and did not find expression in the final deposit. In a second experiment, a 3-cm-thick layer of flour was introduced into the horizontal runout path. Digitate development of the flow front was more pronounced in this run, which we attribute to enhanced flow perturbation as the sand encountered deformable and erodible substrate conditions (Fig. 3C). Lobes wider than the original flow front irregularities were preserved in the deposit as a consequence of more material overriding already stationary sand and flow front spray developing. Runout was shorter than in the metal surface case; and substrate erosion, entrainment, and bulldozing were observed. In this qualitative experiment, which simply served to demonstrate the universality of longitudinal flow feature development, no attempt was made to relate the experimental scale to that of field phenomena.

In summary, all free-surface granular flows apparently have the potential for large-scale longitudinal flow structures that correspond in relative scale and location with ridges. The conditions under which granular flows can be expected to develop prominent longitudinal ridges appear to include:

(i) presence of angular grains and a nonuniform grain size distribution;
(ii) dry or saturated flows;
(iii) rigid or erodible substrate;
(iv) high-velocity flows.

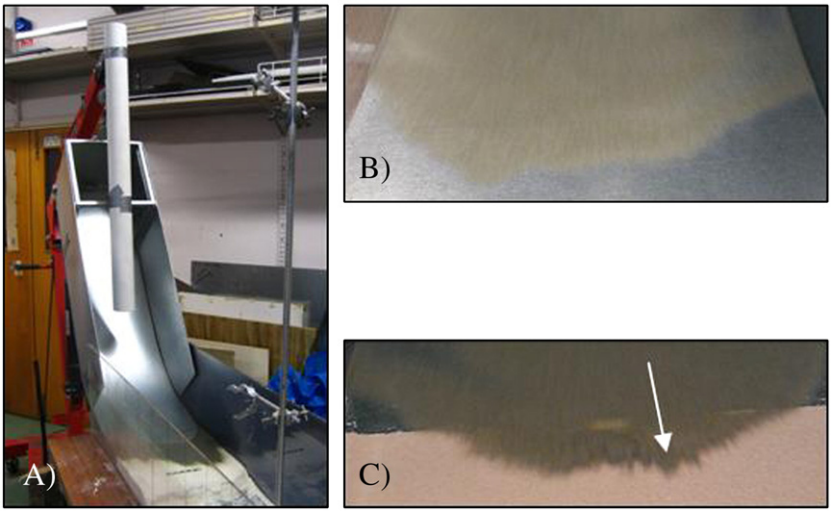


**Fig. 3.** (A) Experimental setup used in the small-scale sand avalanche experiments. The white tube is 1m long through which the sand was fed unto the metal slope (angle of 60°). This slope gradually decreases in steepness into the horizontal runout plane. In (B) this plane consisted of metal and minute longitudinal features were observed at the avalanche front during flow. In the setup shown in (C) a layer of flour was introduced, simulating rough erodible substrate conditions. These caused enhance flow front perturbations and lead to more pronounced ridging in the flow, which found expression in digitate flow fronts. Flume width is 30cm.

These include all the mass movement situations in which longitudinal ridging has been reported in the field and in the laboratory.

## 4. Data collection

During the course of an ongoing investigation of rock and debris avalanche dynamics, a database currently containing close to 400 volcanic and non-volcanic avalanche deposits world-wide is being prepared. Deposit descriptions and statistics are distilled from the literature, such as deposit volume, area, runout, drop height, thickness, etc. Included are the deposit's morphology and texture, data on its source area, pre-avalanche topography, substrate involvement and type of deformation, and many other descriptive features. Within this data array we noticed the repeated mentioning of longitudinal morphological features and we selected the best described deposits with the most complete dataset for hummock, ridge and flowband dimensions for discussion in the next section of this paper. Our research was further extended to snow and ice avalanches, and pyroclastic and block-and-ash flows published in the literature.

## 5. Case studies

In Table 2, a number of well described rock and debris avalanche deposits that feature longitudinal ridges, flowbands, radially aligned hummocks and digitate flow fronts are listed with their respective authors and dates of publication for reference. In the following we briefly describe a selected group of these deposits to illustrate their features and give an overview of their general deposit characteristics.

### 5.1. Radially-aligned hummocks in volcanic debris avalanches

Sector collapse of Jocotitlán volcano, México, resulted in the emplacement of a clast-supported debris avalanche with large conical hummocks in the proximal reaches and smaller clusters of hummocks in the distal reaches of the western depositional area (Siebe et al., 1992). These hummocks are all aligned radially with respect to the source (Fig. 4). The eastern depositional area is block-slide controlled and exhibits a different and partially buried topography. Clast sizes everywhere range from a few centimetres to several tens of meters in diameter. The deposit lacks fine, weak pyroclastic and hydrothermally altered materials, and was emplaced onto (most likely saturated) lacustrine and volcaniclastic sediments.

Hummocks in the 1980 Mount St Helens, Washington, debris avalanche deposit are elongated and oriented dominantly parallel to flow direction (Glicken, 1986). Siebert et al. (1995) observed that at the Burr Point debris avalanche of Augustine volcano, Alaska, proximal hummocks are aligned radial to source, whereas distal hummocks show a transverse orientation where the avalanche has entered the sea. These authors further state that debris avalanches at other volcanoes also display a predominance of radially aligned hummocks.

### 5.2. Prominent elongate ridges in rock avalanches

The Round Top (New Zealand) rock avalanche (Wright, 1998; this study) was sourced in mylonitic schist of the Alpine Fault area. It is mainly clast-supported in the proximal reaches with blocks up to 2–3m long axis and grades into finer material in the distal reaches with

**Table 2**
List of subaerial rock and debris avalanche deposit features

| Deposit name and location | Deposit type | Longitudinal ridges | Flowbands | Aligned hummocks | Lobate/digitate front | Reference |
|---|---|---|---|---|---|---|
| Acheron, New Zealand | RA | x | | | | Smith et al. (2006) |
| Adair Park Breccia, US-Arizona | RA | x | | | | Yarnold and Lombard (1989) |
| Altenau, Germany* | RA | x | | | x | von Poschinger (1994) |
| Black Rapids Glacier, US-Alaska* | RA | | x | | | Jibson et al. (2006) |
| Blackhawk, US-California | RA | x | | x | | Johnson (1978) |
| Carlson, US-Idaho | RA | x | | | | Shaller (1991) |
| Dulung Bar-Darkot, Pakistan | RA | x | | | x | Hewitt (2006) |
| Fernpass | RA | x | | | | Abele (1964) |
| Flims, Switzerland | RA | x | | | x | von Poschinger et al. (2006) |
| Ganges Chasma, Mars | RA | | x | | | Lucchitta (1978) |
| Ghoro Choh I, Pakistan* | RA | x | | | x | Hewitt (2006) |
| Ghol-Ghone B, Pakistan | RA | x | | | x | Hewitt (2006) |
| Marquartstein, Germany | RA | x | | | x | von Poschinger (1994) |
| Mink Creek, Canada | RA | x | | | x | Geertsema et al. (2006) |
| Mt Munday, Canada | RA | | x | x | x | Evans and Clague (1998) |
| Pink Mountain, Canada | RA | x | | x | | Geertsema et al. (2006) |
| Round Top, New Zealand* | RA | x | | x | x | Wright (1998); this study |
| Sherman Glacier, US-Alaska* | RA | | x | x | x | McSaveney (1978) |
| Unnamed Gobi Desert, Mongolia | RA | x | | | | This study |
| Val Pola, Italy | RA | x | x | | | Crosta et al. (2004) |
| Aucancilcha, Chile | VDA | x | | x | x | Francis and Wells (1988) |
| Augustine (Burr Pt), US-Alaska* | VDA | | | x | x | Siebert et al. (1995) |
| Chimborazo, Ecuador | VDA | x | | | x | Siebert (1984), Bernard et al. (2008) |
| Dikii Greben, Kamchatka | VDA | x | | | | Ponomareva et al. (2006) |
| El Estribo, Mexico | VDA | x | | | | Capra et al. (2002) |
| Harimkotan | VDA | | x | | | Belousov et al. (1999) |
| Jocotitlan, Mexico* | VDA | x | | x | | Siebe et al. (1992); this study |
| Lastarria, Chile* | VDA | | x | x | x | Naranjo and Francis (1987) |
| Llullaillaco, Argentina* | VDA | x | x | x | x | Richards and Villeneuve (2001) |
| MSH, US-Washington* | VDA | x | | x | | Glicken (1986) |
| Ollague, Chile/Bolivia | VDA | x | | | | Clavero et al. (2004) |
| Parinacota, Chile | VDA | x | | | x | Clavero et al. (2002) |
| Popcatepetl, Mexico | VDA | x | | | x | Robin and Boudal (1987) |
| Shiveluch (1964), Kamchatka | VDA | | x | | | Belousov et al. (1999) |
| Socompa, Chile | VDA | x | | | | Van Wyk De Vries et al. (2001) |
| Taunshit, Kamchatka | VDA | | x | | | Belousov et al. (1999) |
| Unzen (1792), Japan | VDA | x | | x | | Siebert (2002) |

Deposits with '*' are discussed in Section 5 of the text. RA = rock avalanche, VDA = volcanic debris avalanche.

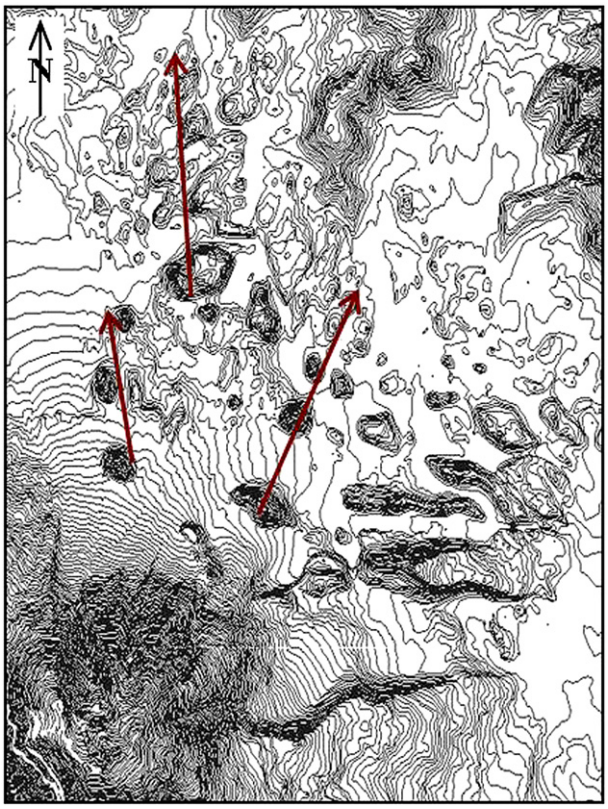


**Fig. 4.** Example of hummock alignment in volcanic debris avalanches, Jocotitlán, Mexico. Distance horizontally across image is ~ 9km.

remnant source stratigraphy preserved in the deposit fabric. Large (several hundred metres long and 10–30m high) elongate ridges are found in the proximal–medial area (Fig. 5A), whereas smaller hummocks (aligned with ridge long axes) and digitate emplacement characterise the distal reaches. The avalanche was emplaced onto saturated floodplain gravels, and bulldozed substrata are found at ridge toes.

Very similar observations of radial elongate ridge orientation and associated substrate bulldozing at ridge termini have been reported from numerous rock avalanches in the Karakoram Himalaya (Hewitt, 2006s; Fig. 5B), and the Altenau (von Poschinger, 1994; Fig. 5C) rock avalanches in Germany.

### 5.3. Flowbands in rock avalanches emplaced onto glaciers

The Sherman Glacier rock avalanche, Alaska, has long flowbands and digitate flow fronts (Fig. 6A, data from McSaveney, 1978 and Nicoletti and Sorriso-Valvo, 1991). It was sourced in sand- and siltstones and entrained snow, ice, soil, and till. Tracing the furrows between the ridges back toward source shows that many contain a large boulder at their "beginning point" (M.J. McSaveney, GNS Science, NZ, personal communications, 2007). Some ridges of rock avalanches emplaced onto glaciers also have large clasts at their distal ends (Evans and Clague, 1998).

A moment magnitude 7.9 earthquake on the Denali Fault, Alaska, in 2002 triggered thousands of small and large landslides (Jibson et al., 2006). The most spectacular avalanches were emplaced onto the Black Rapids Glacier. They are unusually thin (3m) for their volume ($37 \times 10^6 m^3$), overtopped a 50-m-high moraine at velocities of over 130km/h, travelled long distances on a slope of 1–2°, and show sharp margins and long flow-parallel furrows and ridges (flowbands).

### 5.4. Flowbands and striations in volcanic debris avalanches

The Lullaillaco volcanic debris avalanche in Argentina (Richards and Villeneuve, 2001) has two major lobes where the flow divided around a cone and travelled down two parallel valleys. It generally lacks larger boulders and was most likely emplaced hot. The northern lobe is striated and sunk into the distal salt flats. The southern lobe has prominent longitudinal ridges and a distal raised toe where it encountered but did not sink into the salt flats. Striations like the ones on Lullaillaco's northern lobe are also the characteristic feature of the 1964 Shiveluch debris avalanche (Belousov et al., 1999; Fig. 6B). They extend along the entire flow length and are deformed or disintegrated into a hummocky surface where motion was impeded.

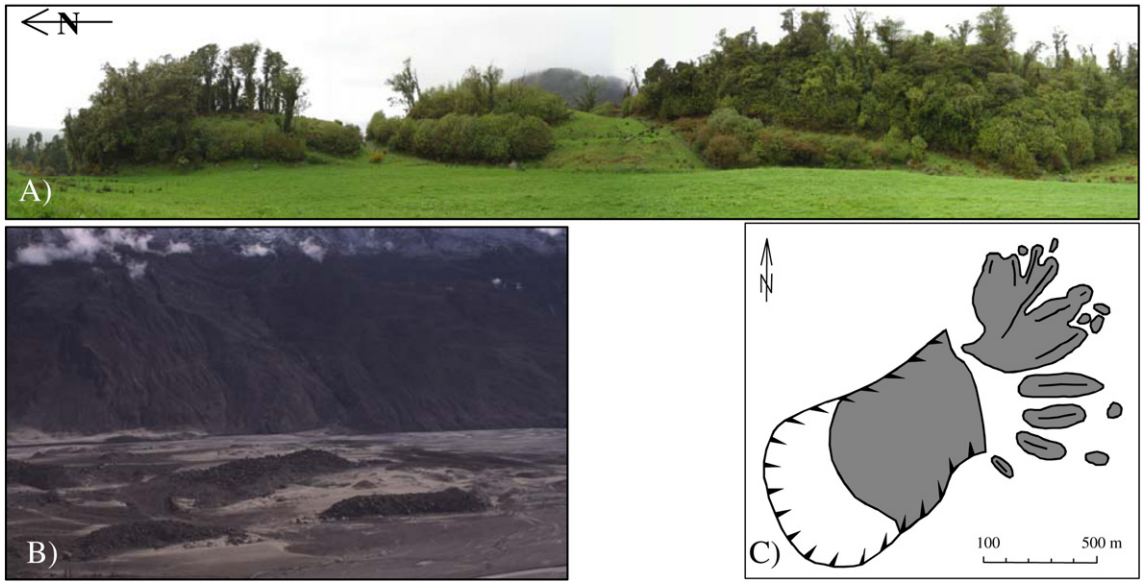


**Fig. 5.** (A) One of several elongate ridges aligned radial to source in the Round Top rock avalanche deposit, West Coast, New Zealand (ridge segment shown is ~ 350m long). (B) Longitudinal ridges (on the order of 35m in height) in the Ghoro Choh I rock avalanche deposit, Karakoram Himalayas, Pakistan (image courtesy of Ken Hewitt). (C) Simplified mophological map of the Altenau rock avalanche, Germany (modified from von Poschinger 1994) showing ridge elongation and flow direction.

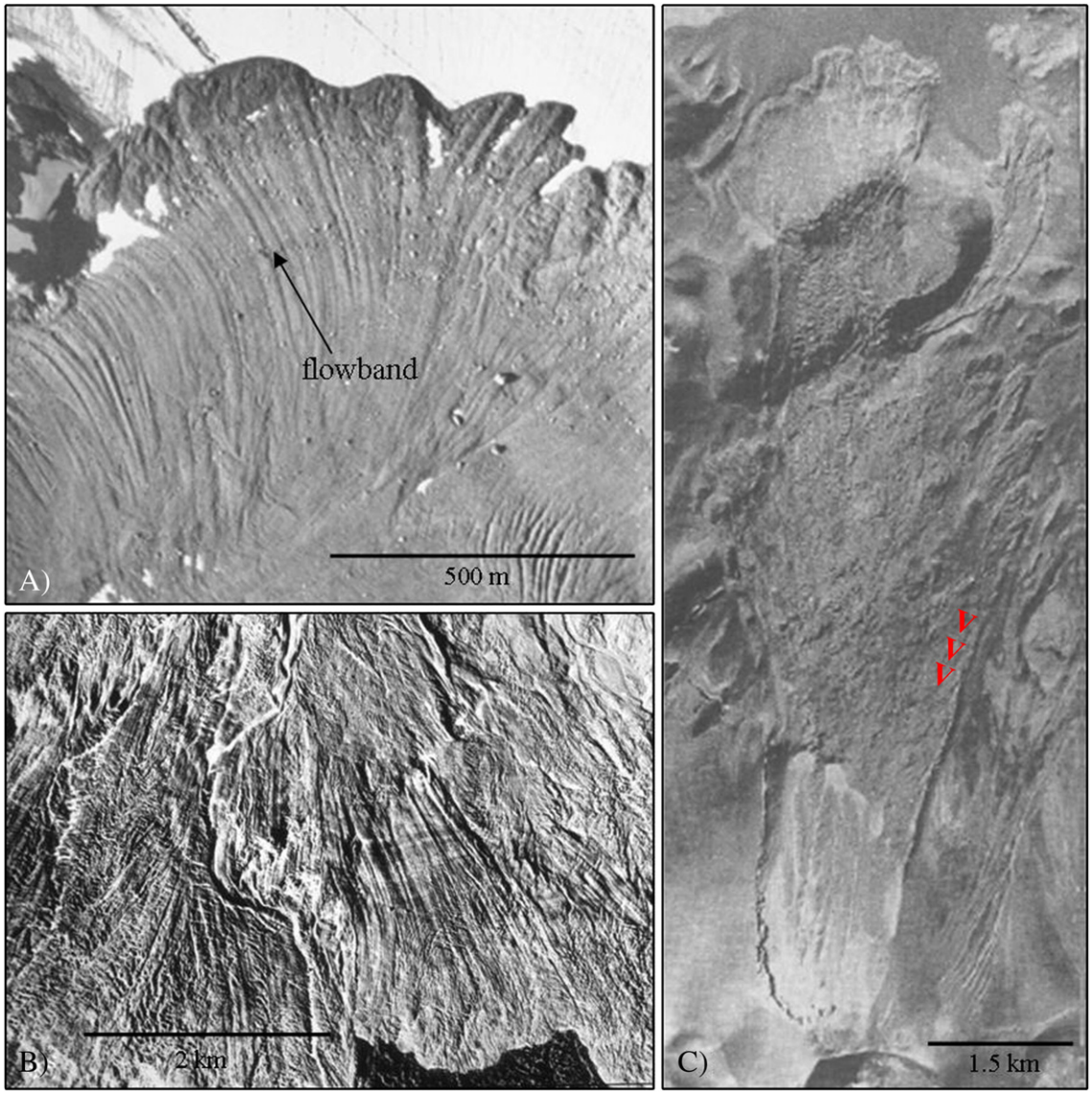


**Fig. 6.** Flowbands in rock and debris avalanche deposits. (A) Part of the Sherman Glacier rock avalanche, Alaska (image courtesy of Mauri McSaveney) showing typical flowbands. (B) Striated surface of the 1964 Shiveluch debris avalanche (image courtesy of Alexander Belousov and Marina Belousova). (C) The high-velocity Lastarria volcanic debris avalanche (Naranjo andFrancis 1987; image reproduced with permission from publisher) features so-called "herringbone" flowbands.

At Lastarria volcano, Chile, the debris avalanche initiated along bedding planes of weak pyroclastic material and created a lobate to digitate deposit that spread only 38° laterally (Naranjo and Francis, 1987). It displays longitudinal ridges with "herringbone" structures similar to those found in ejecta sheets and is entirely composed of mechanically weak pyroclastic material (Fig. 6C). Its estimated emplacement velocity was 180–300km/h.

### 5.5. Longitudinal features in submarine debris avalanches

Surface morphologies of submarine debris avalanches are often complicated by secondary turbidites and flow channels in the margin runoff zone, leaving their interpretation for longitudinal features ambiguous. Nevertheless, examples of linear flow structures, elongate blocks aligned parallel to flow direction, and aligned hummocks include, for example, the debris avalanches from Dominica Island, Lesser Antilles Arc (Deplus et al., 2001), offshore Angola (Gee et al., 2006), the Alika 2 off Hawai'i (Moore and Chadwick, 1995), and the La Orotava DA off Tenerife (Huerlimann and Ledesma, 2003).

### 5.6. Flowbands and digitate emplacement of pyroclastic flows and block-and-ash flows

The 1993 eruption of Lascar volcano, Chile, produced a series of pyroclastic flow deposits (e.g., Sparks et al., 1997; Fig. 7A) with typical finer grained basal layers and coarse clast concentration towards the top and margins. They contain both pumice-rich and lithic-rich facies. The lithic-rich facies is mainly confined to deposit interiors, and lithic-rich deposits were observed on slopes of 6–14°. Pumice-rich facies, on the other hand, typically occur at the margins and distal parts of the pyroclastic flow fans, and pumice-rich deposits were observed only on slopes of < 4°. Curving digitate emplacement is prominent in the flow fans.

Block-and-ash flows from the 1990 to 1995 Unzen (Japan) eruption (Miyabuchi, 1999) exhibit lobate/digitate flow fronts and lateral levees in valley paths. The deposits have unconsolidated ash matrices and blocks up to 10m in diameter. They were emplaced hot, contain gas escape pipes, and have fine-grained basal and coarse depleted marginal flow units. The estimated total volume (dry rock equivalent) of the block-and-ash flow and talus apron is $1.2 \times 10^8 m^3$.

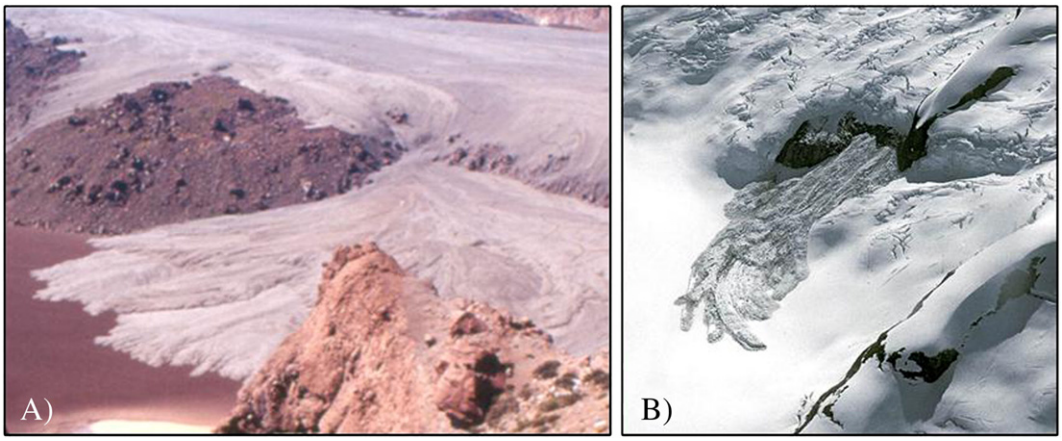


**Fig. 7.** Flowbands and digitate deposit shapes in (A) the Lascar pyroclastic flow, Chile (flow fan is approximately 200m across; image courtesy of Karim Kelfoun) and (B) the Juneau Icefield, Canada (avalanche is about 500m long; image courtesy of Scott McGee).

*5.7. Flowbands and digitate features in snow and ice avalanches*

Morphological studies of snow and ice avalanches are far and few between, but several images from the literature and the web show longitudinal ridging and digitate shapes (Fig. 7B) of many snow and ice avalanche deposits (e.g., Jomelli and Bertran, 2001; McClung and Schaerer, 2006; Pralong and Funk, 2006).

Data collected from dry and damp snow avalanches in the Wasatch Mountains of Utah and from the Chugach Mountains of south-central Alaska during the winters of 1975 through 1979 revealed longitudinal shear planes as the most striking features of many deposits (Mears, 1980). Transverse shear planes were observed in the decelerating parts of the flows. Shear planes in snow avalanches find expression in surficial ridges or, were exposed, as steeply dipping planes like those of faults; they are thought to result from differential motion of the snow pack, and occur in both confined and unconfined runout zones (Mears, 1980).

*5.8. Ejecta sheets and planetary landslide deposits*

Ejecta sheets are often found surrounding Martian and Lunar impact craters. Some are striated, others look more fluid-like with radial digits that seem to have raised toes (e.g., Lunae Planum, Mars; Barnouin-Jha et al., 2005).

Landslides on the extraterrestrial planets resemble their terrestrial counterparts and are sometimes compared to the Sherman

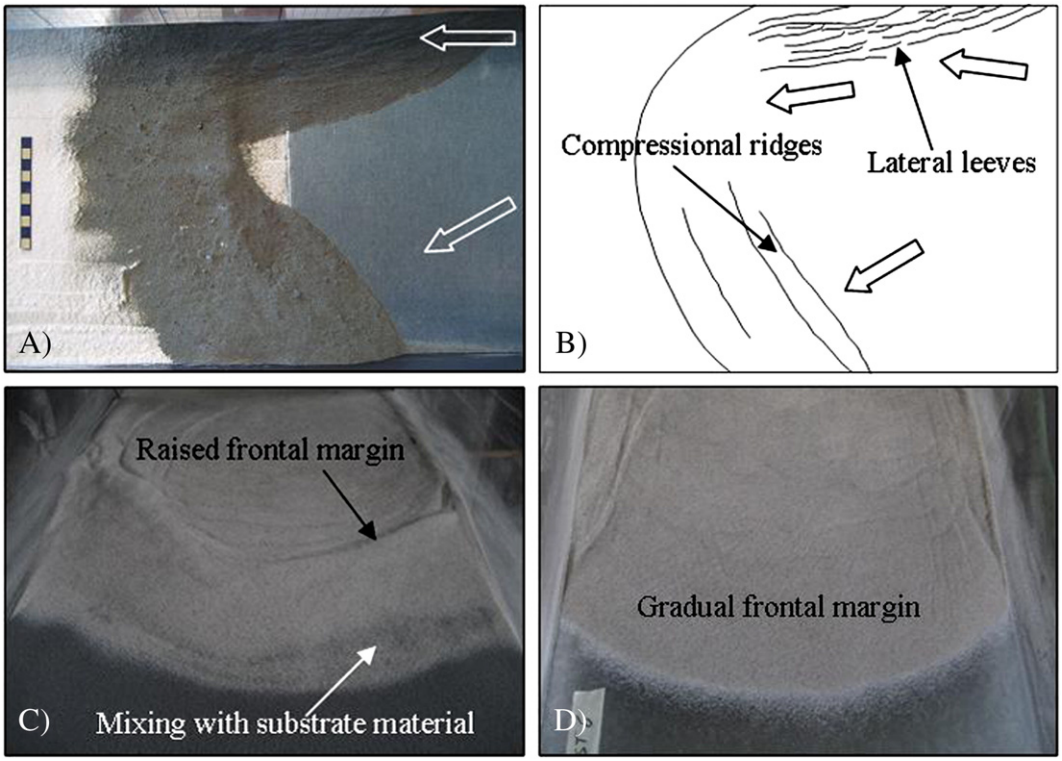


**Fig. 8.** (A) Lateral levees developed in a small sand avalanche experiment where flow was parallel to the confining walls (in top part of image), whereas compressional ridges formed in response to deceleration in the lower depositional area. The sand was released down a metal chute and ran out over a 3cm thick layer of dry flour. (B) Conceptual sketch showing the main flow directions (arrows) and features. (C) Raised flow front of sand avalanche encountering a thin layer of erodible substrate (black sand). (D) Sand avalanche emplaced onto zero friction, undeformable substrate (smooth metal) exhibits gradual flow front thickness decrease. Flume width is 30cm.

Glacier rock avalanche (e.g., Ganges Chasma and Coprates Chasma on Mars; Lucchitta, 1979; Quantin et al., 2004) attesting to their commonly striated/ridged morphology. A particularly interesting feature of a number of Martian deposits is the fact that the divergence angle of the striations increases with distance from source, perhaps indicating a constant divergence velocity as longitudinal velocity decreases. This is also apparent in the pattern of the Sherman Glacier deposit (Fig. 6A).

## 6. Other surface morphologies

Other morphological features of granular flow deposits include transverse ridges and lateral levees (Fig. 8A, B). These features differ fundamentally from longitudinal ridges, which are extensional, flow-parallel phenomena. Transverse ridges, on the other hand, are usually compressional and are mainly associated with flow deceleration where a change in surrounding or underlying medium increases frictional resistance or absorbs flow momentum, and they appear predominantly in the distal deposit reaches where they also find expression as raised distal margins (Fig. 8C). Examples include flow into a body of water (e.g., the Unzen, 1972 volcanic debris avalanche deposit, with a change from subaerial elongate ridges to submarine transverse ridges; Siebert, 2002); encounters with soft, deformable substrates (e.g., Mombacho (Shea et al., 2008) and Ollagüe (Clavero et al., 2004) volcanic debris avalanche deposits), or decrease in topographic gradient (e.g., Blackhawk rock avalanche; Johnson, 1978). Lateral levees are common features of avalanches emplaced into narrow valleys and result from flow interaction with the dry, sloping valley walls [e.g., the Acheron rock avalanche (Smith et al., 2006) has lateral levees along the valley path but these disappear where the lateral confinement ends]. They occur in snow avalanches because of lateral interaction with stationary snow cover, and in some flows result from the preferential accumulation of coarse, higher-friction debris at the free surface (Johnson, 1978), which is also common in debris flows.

## 7. Discussion

From the preceding presentation of longitudinal morphological features on the surfaces of naturally occurring mass movement deposits, and their small-scale laboratory counterparts, we learned that they can form in a variety of materials, at a range of emplacement velocities and on different scales. The following is a summary relating the observed deposit features with the properties of the materials involved:

(i) High elongate ridges develop in strong, competent, high friction material, sometimes with a mechanically weak base, i.e., significant substrate involvement such as loose saturated material (rock avalanches on valley fill etc. some volcanic debris avalanches).
(ii) Aligned hummocks in the distal reaches of avalanche deposits appear to develop as a consequence of extensional ridge breakup, when the frontal parts of the ridges have greater velocity/momentum than the rear, which starts depositing earlier or is halted by locally bulldozed substrates.
(iii) Aligned hummocks throughout volcanic debris avalanches form if the source material is strong and competent (i.e., lacks weak pyroclastic or hydrothermally altered material) and the deposit is relatively thick with respect to the width of their basal shear layer (see below).
(iv) Flowbands develop in weak (low density, loose, small clast sizes, highly brittle) source material (snow avalanches, loose volcanic debris avalanches made up of, e.g., pumice or hydrothermally altered fine material, pyroclastic flows) or in fragmented material on a fluidised substrate (rock avalanches on glaciers where basal friction is low), leading to an increase in velocity accompanied by rapid deposit thinning.
(v) In other cases, flowbands are the result of high-velocity emplacement of materials with relatively small clast sizes (some volcanic debris avalanches, pyroclastic flows, ejecta sheets).

Apparently, a relationship involving emplacement velocity, bulk/material density, and frictional behaviour (clast angularity) controls the degree to which prominent longitudinal features form in granular flows from the universal tendency to longitudinal ridging present in all grain flows. Interaction of the mass movement with its substrate furthermore influences avalanche behaviour and ridge/flowband development and preservation.

### 7.1. Emplacement velocity

Flowbands are most prominent in the high-velocity emplacement of, e.g., ejecta sheets (or the unusual Lastarria debris avalanche), in rock avalanches emplaced onto glaciers (e.g. Sherman Glacier, Black Rapids Glacier), and in snow and ice avalanches (e.g. Juneau Icefield). Where avalanche material moved fastest in the longitudinal flow direction, with material moving much more slowly laterally, ridge and flowband formation is favoured (Fig. 9A). An example is the Lastarria volcanic debris avalanche with its very directed emplacement (narrow spreading angle of 38°), high emplacement velocity and prominent flowbands in the final deposit. Hungr and Evans (2004) have shown statistically that rock avalanches emplaced onto glaciers travel further distances than those on other materials. These avalanches have the ability to override substantial topographic obstacles at high velocities (e.g. Black Rapids Glacier), are unusually thin and have flowbands as their characteristic surface feature. With more rapid sideways motion (lateral velocity approaches longitudinal velocity), hummocks and ridges tend to break up into clusters (Fig. 9B). This is the case in the decelerating, spreading distal parts of many rock and debris avalanches. As the lateral velocity increases further with respect to longitudinal velocity, hummocks will become more scattered (Fig. 9C).

Sudden deceleration (e.g., from an encounter with deformable substrates) will lead to the formation of compressional ridges or raised flow fronts (e.g. Mombacho, Ollagüe). Where flow takes place relative to stationary lateral material, the high-velocity gradient will slow the avalanche material at the sides and lead to the formation of lateral levees (e.g. Acheron).

Small, low-velocity avalanches show compression-dominated surface features. In these cases, avalanche runout distance complies with simple frictional behaviour, similarly to small sand avalanches emplaced onto rough, unerodible surfaces (e.g., Davies and McSaveney, 1999). In these latter cases, the *tendency* for longitudinal feature formation can be observed on very small scales, but their development is impeded. This means that minute longitudinal features are visible in these simple granular flows in the form of undulating surfaces or irregular frontal margins; but no immediately obvious flowbands, ridges, or digits/lobes have developed in the deposit.

### 7.2. Material properties

The maximum steepness of a static granular pile is controlled by the material's angle of internal friction; this is higher for angular grains than for rounded ones. The ability of a pile to retain steepness while being transported as part of a mass movement depends also on the extent to which flow-induced vibrations affect it. The same applies to the cross-sectional steepness of a ridge or hummock. During runout, therefore, two opposing tendencies are present; the intrinsic tendency of a granular flow to form ridges or hummocks and the tendency of flow motion to flatten them. On this basis we would expect ridges to be relatively less steep-sided in shallower flows because the vibrations

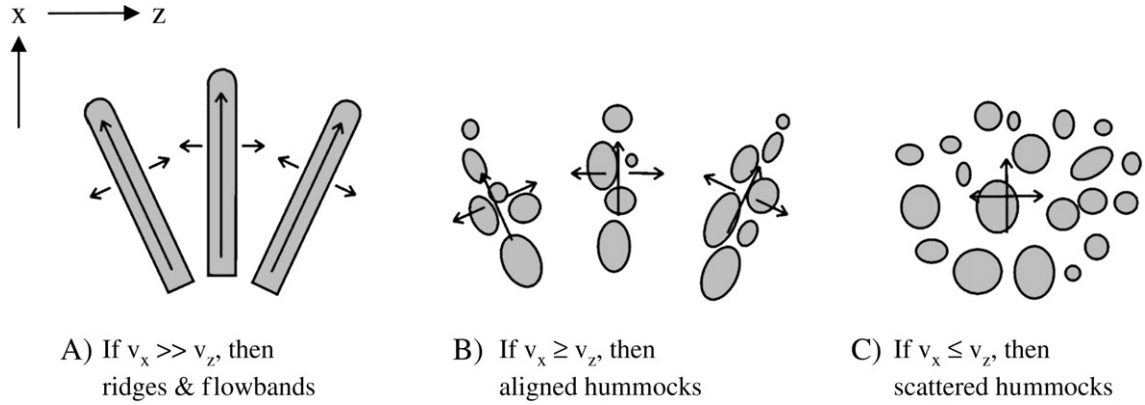


**Fig. 9.** Influence of velocity distribution and direction on the formation of elongate ridges versus aligned or scattered hummocks. vx = velocity in flow direction, vz = velocity perpendicular to flow direction. This can apply to the deposit as a whole or to individual areas alone (e.g. lobes, distal versus proximal).

from substrate interaction would be greater; this would also be the case in more distal regions. Apparently, mechanically strong, competent, high friction material also should favour the formation of longitudinal ridges and aligned hummocks of substantial sizes (in rock and volcanic debris avalanches 10–100s m height, e.g. Jocotitlán). By contrast, deposits comprising mechanically weak, loose, low density, lower friction material and smaller clast sizes tend to have long, thin flowbands (e.g. Llullaillaco, Lastarria, Lascar), which, by observation, are less steep than the ridges formed in strong, high friction materials.

Detailed investigation of several hundred hummocks of the 1980 Mount St. Helens debris avalanche showed that block facies hummocks with no matrix facies (type 'A' hummocks) are generally much larger and steeper than those that are made up entirely of matrix facies (type "B"); Glicken, 1986. Furthermore, unusually steep conical hummocks of the proximal Jocotitlán DA lack fine material and consist entirely of large, angular dacite blocks.

### 7.3. The influence of basal geometry on hummock/ridge size

We identify two distinct types of shear in debris avalanches:

(i) Where the shear is concentrated at the base of the avalanche, because of weak substrate or saturated basal material, we call *basally weak*. This appears to be the case in many volcanic debris avalanches and, in general, where the avalanche is widely relative to its depth. In basally weak situations, shear is concentrated in the basal region of the mass movement. If the overlying material is weakly cohesive, as in volcanic debris avalanches, the tendency for the shearing layer to spread longitudinally and laterally will cause the overlying material to fail passively in extension. This will give rise to block-like failures in the extending material, causing ridges and/or hummocks.

(ii) Where the shearing is distributed more or less uniformly through the flow depth, apart from a thin (~ 10m) carapace of coarse blocky material, we call *basally strong*. This occurs in many dry rock avalanches where the flow is relatively deep and applies to the nonfragmenting carapace (Dunning, 2004) of a basally strong rock avalanche; this is an ~ 10-m-deep layer in which stresses are insufficient to prevent grain bridges from failing by buckling, so little fragmentation occurs and apparent friction is normal. This layer will again fail passively in extension as the fragmenting substrate spreads, giving rise to hummocks or ridges (McSaveney and Davies, 2007).

In both cases, the size of the hummocks or ridges is expected to scale with the depth of the passive layer. Hence, we expect the hummocks on a basally weak avalanche to be relatively larger than

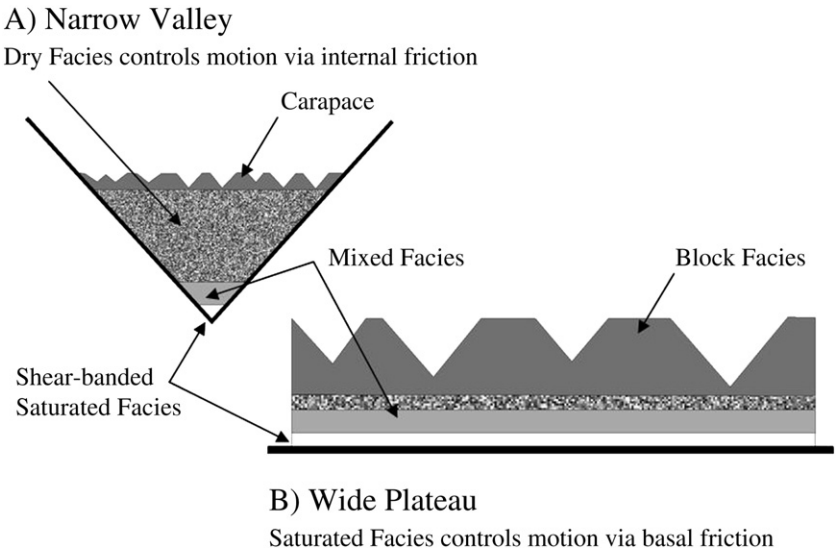


**Fig. 10.** Flow cross-sections illustrating hummock size dependence on basal shear zone width. (A) Emplacement into narrow valley in which case the internal avalanche friction has more influence on avalanche motion and morphology development than the relatively narrow basal shear zone (e.g. typical rock avalanche environment). (B) Case of open runout onto wide plains in which case larger hummocks can form in response to the greater influence of the basal shear in controlling avalanche motion.

those on basally strong avalanches because the depth of the passive layer in the latter is shallower than in the former (Fig. 10). Field data (e.g., Glicken, 1986; Evans et al., 1994) show that this is indeed the case. Evidence is also available that the size of hummocks decreases with distance from the avalanche source (LeCorvec, 2005), which is to be expected as the depth of the upper nonshearing layer decreases with increased area because of spreading.

### 7.4. Substrate influence

When large amounts of saturated substrate material are entrained into a rock/debris avalanche, transformation into more mobile debris flows can occur leaving characteristically thinner and flatter-topped deposits. Smaller amounts of entrainment on the other hand can alter basal compositions and mechanical behaviour, thus influencing overall avalanche emplacement processes. For example, rock avalanches emplaced onto glaciers sometimes appear to be emplaced at high velocity. Snow, ice, and water are mixed into the basal rock avalanche material, fluidizing it and thus reducing its frictional resistance to flow. This could lead to ridges "stretching" into flowbands as there are no obstacles to halt their motion nor are the flows thick enough to generate hummocks.

Flow front perturbations in any granular flow through an encounter with or entrainment of larger obstacles, overriding of a rough surface, or local deposition of larger avalanche boulders can intensify ridge/lobe/digit development (e.g., Sherman Glacier, Fig. 6A), or laboratory analogue models (e.g. Pouliquen and Vallance, 1999; this study).

An encounter with deformable substrates can locally create hindrances, inhibiting avalanche motion. For example, local bulldozing of substrates beneath an advancing avalanche ridge can impede its advance, leading to compressional features within the ridge and prevention of ridge breakup into hummocks, thus preserving the feature in the deposit (e.g. Round Top, Ghoro Choh I, Altenau). In other cases, the deformable substrate (and also motion into water; e.g. Unzen) can drastically slow the avalanche front leading to the formation of flow-transverse compressional ridges (e.g. Mombacho, Ollagüe).

### 7.5. Feature formation differences in the laboratory and in nature

In the laboratory, ridges and lobes form because of grain size segregation and flow front perturbations. This leads to accumulation of larger grains in the longitudinal section, while the finer material continues to move downslope; i.e., this segregation of larger clasts at the flow front causes local flow front perturbation and encourages distinct lobe (ridge) formation. However, uniformly graded, angular material also creates frontal lobes, and we hence do not regard grain size segregation as a necessary process for the initiation of lobes or ridges — particularly since, in the field, such grain size distributions/segregations are rarely observed. Typically, no velocity difference is noted between adjacent ridges, and lithologies extend across them unperturbed from their original location (i.e., no segregation or lateral sorting/rearrangement occurs; e.g., Belousov et al., 1999).

Dufresne (in preparation) presents evidence that laboratory subsurface features correspond with those in the field, at least qualitatively; and this supports our suggestion of significant correspondence between field and laboratory surface features.

## 8. Conclusions

This is an exploratory study of the occurrence and significance of longitudinal surface features in mass movement granular flows. We have identified significant similarities of longitudinal features in mass movement deposits in a very wide range of materials and settings, and we also related the range of feature types (hummocks, ridges, flowbands) to the flow conditions they appear to be largely associated with. We have shown that the formation of longitudinal ridges is an intrinsic process of free-surface granular flows and that the expression of this process as ridges, flowbands, or aligned hummocks at the surface of large-scale mass movement deposits largely depends upon:

(i) the frictional behaviour of the material i.e., its ability to resist internal deformation and the presence of angular clasts with varying grain sizes;
(ii) the emplacement velocity and direction;
(iii) the emplacement geometry and flow cross section; and
(iv) the influence of substrates on the flow dynamics.

Furthermore, processes such as burial or erosion by secondary flows play a crucial role in the preservation of longitudinal features.

Despite the great variety of geological materials forming avalanches and their equally great variety of proposed emplacement dynamics and conditions (rock avalanches, large volcanic debris avalanches, hot pyroclastic flows, snow and ice avalanches, high-velocity ejecta sheets and blast deposits, small-scale laboratory sand avalanches, etc.), the observation that they all share the same family of characteristic surface features indicates that there is considerable potential for further development of this topic, as the longitudinal features provide definite information on flow direction and could provide insights into emplacement processes of granular materials in general.

## References


Abele, G., 1964. Die Fernpasstalung und ihre morphologischen Probleme. Tubiner Geograpgische Studien 12, 123.

Anthony, J.L., Marone, C., 2005. Influence of particle characteristics on granular friction. Journal of Geophysical Research B: Solid Earth 110 (8), 1–14.

Aranson, I.S., Malloggi, F., Clément, E., 2006. Transverse instability of avalanches in granular flows down an incline. Physical Review E — Statistical, Nonlinear, and Soft Matter Physics 73 (5), 4 pages.

Barnouin-Jha, O.S., Baloga, S., Glaze, L., 2005. Comparing landslides to fluidized crater ejecta on Mars. Journal of Geophysical Research E: Planets 110 (4), 1–22.

Belousov, A., Belousova, M., Voight, B., 1999. Multiple edifice failures, debris avalanches and associated eruptions in the Holocene history of Shiveluch Volcano, Kamchatka, Russia. Bulletin of Volcanology 61 (5), 324–342.

Bernard, B., van Wyk de Vries, B., Barba, D., Leyrit, L., Robin, C., Samaniego, P., 2008. The Chimborazo sector collapse and debris avalanche: deposit characteristics as evidence of emplacement mechanisms. Journal of Volcanology and Geothermal Research 176 (1), 36–43.

Capra, L., Macías, J.L., Scott, K.M., Abrams, M., Garduño-Monroy, V.H., 2002. Debris avalanches and debris flows transformed from collapses in the Trans-Mexican Volcanic Belt, Mexico — behavior, and implications for hazard assessment. Journal of Volcanology and Geothermal Research 113 (1–2), 81–110.

Clavero, J., Sparks, R., Huppert, H., Dade, W., 2002. Geological constraints on the emplacement mechanism of the Parinacota debris avalanche, Northern Chile. Bulletin of Volcanology 64 (1), 40–54.

Clavero, J., Polanco, E., Godoy, E., Aguilar, G., Sparks, R.S.J., van Wyk de Vries, B., de Arce, C.P., Matthews, S., 2004. Substrata influence in the transport and emplacement mechanism of the Ollagüe debris avalanche (Northern Chile). Acta Vulcanologica 16 (1–2), 59–76.

Crandell, D.R., Miller, C.D., Glicken, H.X., Christiansen, R.L., Newhall, C.G., 1984. Catastrophic debris avalanche from ancestral Mount Shasta Volcano, California. Geology 12 (3), 143–146.

Crosta, G.B., Chen, H., Lee, C.F., 2004. Replay of the 1987 Val Pola Landslide, Italian Alps. Geomorphology 60 (1–2), 127–146.

Davies, T.R., McSaveney, M.J., 1999. Runout of dry granular avalanches. Canadian Geotechnical Journal = Revue Canadienne de Geotechnique 36 (2), 313–320.

Deplus, C., Le Friant, A., Boudon, G., Komorowski, J.C., Villemant, B., Harford, C., Segoufin, J., Cheminee, J.L., 2001. Submarine evidence for large-scale debris avalanches in the Lesser Antilles Arc. Earth and Planetary Science Letters 192 (2), 145–157.

Dufresne, A., (in preparation). The influence of runout path material on rock and debris avalanches: field evidence and analogue modelling. Unpublished Ph.D. thesis. Canterbury University, Christchurch, New Zealand.

Dunning, S. (2004). Rock avalanches in high mountains. Unpublished Ph.D. thesis. University of Luton, England.

Evans, S.G., Clague, J.J., 1998. Rock avalanche from Mount Mundy, Waddington Range, British Columbia, Canada. Landslide News 11, 23–25.

Evans, S.G., Hungr, O., Enegren, E.G., 1994. The Avalanche Lake rock avalanche, Mackenzie Mountains, Northwest Territories, Canada; description, dating, and dynamics. Canadian Geotechnical Journal = Revue Canadienne de Geotechnique 31 (5), 749–768.

Francis, P.W., Wells, G.L., 1988. Landsat Thematic Mapper observations of debris avalanche deposits in the Central Andes. Bulletin of Volcanology 50 (4), 258–278.

Francois, B., Lacombe, F., Herrmann, H.J., 2002. Finite width of shear zones. Physical Review E — Statistical, Nonlinear, and Soft Matter Physics 65 (3) 031311/1–031311/7.

Gee, M.J.R., Gawthorpe, R.L., Friedmann, S.J., 2006. Triggering and evolution of a giant submarine landslide, Offshore Angola, revealed by 3d seismic stratigraphy and geomorphology. Journal of Sedimentary Research 76 (1), 9–19.
Geertsema, M., Hungr, O., Schwab, J.W., Evans, S.G., 2006. A large rockslide-debris avalanche in cohesive soil at Pink Mountain, Northeastern British Columbia, Canada. Engineering Geology 83, 64–75.
Glicken, H., (1986). Rockslide-debris avalanche of May 18, 1980, Mount St. Helens Volcano, Washington. Santa Barbara, University of California at Santa Barbara, 98 pp.
Hewitt, K., 2006. Rock avalanches with complex run out and emplacement, Karakoram Himalaya, Inner Asia. In: Evans, S.G., Scarascia-Mugnozza, G., Strom, A.L., Hermanns, R.L. (Eds.), Nato Science Series. Series IV, Earth and Environmental Sciences, Vol. 49, pp. 521–550.
Huerlimann, M., Ledesma, A., 2003. Giant mass movements in volcanic islands: the case of Tenerife. Occurrence and mechanisms of flow-like landslides in natural slopes and earthfills, Sorrento, pp. 105–115.
Hungr, O., Evans, S.G., 2004. Entrainment of debris in rock avalanches: an analysis of a long run-out mechanism. GSA Bulletin 116 (9/10), 1240–1252.
Jibson, R.W., Harp, E.L., Schulz, W., Keefer, D.K., 2006. Large rock avalanches triggered by the M 7.9 Denali Fault, Alaska, earthquake of 3 November 2002. Engineering Geology 83, 144–160.
Johnson, B., 1978. Blackhawk landslide, California, U.S. Rockslides and Avalanches 1, Natural Phenomena. Elsevier, Amsterdam, pp. 481–504.
Jomelli, V., Bertran, P., 2001. Wet snow avalanche deposits in the French Alps; structure and sedimentology. Geografiska Annaler. Series A: Physical Geography 83 (1–2), 15–28.
LeCorvec, N. (2005). Socompa volcano destabilisation (Chile) and fragmentation of debris avalanches. Unpublished M.Sc. thesis. Laboratoire Magma et volcans, Clermont-Ferrand, Universite Blaise Pascal, France. 67 pages.
Lucchitta, B.K., 1978. A large landslide on Mars. Geological Society of America Bulletin 89 (11), 1601–1609.
Lucchitta, B.K., 1979. Landslides in Valles Marineris, Mars. Journal of Geophysical Research 84, 8097–8113.
Mallogi, F., Lanuza, J., Andreotti, B. and Clement, E., (2008). Erosion waves: transverse instabilities and fingering. Soft Condensed Matter (cond-mat.soft). http://arxiv.org/abs/cond-mat/0507163.
McClung, D., Schaerer, P.A., 2006. The Avalanche Handbook. Mountaineers Books, Seattle, WA.
McSaveney, M.J., 1978. Sherman Glacier rock avalanche, Alaska, U.S.A. Rockslides and Avalanches. Elsevier, Amsterdam, pp. 197–258.
McSaveney, M.J., Davies, T.R., 2007. Rockslides and their motion. In: Sassa, K., Fukuoka, H., Wang, F., Wang, G. (Eds.), Progress in landslide science. Springer-Verlag, pp. 113–134.
Mears, A.I., 1980. A fragment-flow model of dry-snow avalanches. Journal of Glaciology 26, 153–163.
Miyabuchi, Y., 1999. Deposits associated with the 1990–1995 eruption of Unzen Volcano, Japan. Journal of Volcanology and Geothermal Research 89, 139–158.
Moore, J.G., Chadwick Jr., W.W., 1995. Offshore geology of Mauna Loa and adjacent areas, Hawaii. Geophysical Monograph 92, 21–44.
Naranjo, J.A., Francis, P., 1987. High velocity debris avalanche at Lastarria Volcano in the North Chilean Andes. Bulletin of Volcanology 49, 509–514.
Nicoletti, P.G., Sorriso-Valvo, M., 1991. Geomorphic controls of the shape and mobility of rock avalanches. Geological Society of America Bulletin 103 (10), 1365–1373.
Ponomareva, V.V., Melekestsev, I.V., Dirksen, O.V., 2006. Sector collapses and large landslides on late Pleistocene–Holocene volcanoes in Kamchatka, Russia. Journal of Volcanology and Geothermal Research 158 (1–2), 117–138.
Pouliquen, O., Vallance, J.W., 1999. Segregation induced instabilities of granular flows. Chaos 9 (3), 621–630.
Pouliquen, O., Delour, J., Savage, S.B., 1997. Fingering in granular flows. Nature 386 (6627), 816–817.
Pralong, A., Funk, M., 2006. On the instability of avalanching glaciers. Journal of Glaciology 52 (176), 31–48.
Quantin, C., Allemand, P., Delacourt, C., 2004. Morphology and geometry of Valles Marineris landslides. Planetary and Space Science 52 (11), 1011–1022.
Richards, J.P., Villeneuve, M., 2001. The Llullaillaco Volcano, Northwest Argentina: construction by Pleistocene volcanism and destruction by sector collapse. Journal of Volcanology and Geothermal Research 105 (1–2), 77–105.
Robin, C., Boudal, C., 1987. A gigantic Bezymianny-type event at the beginning of modern Volcan Popocatepetl. Journal of Volcanology & Geothermal Research 31 (1–2), 115–130.
Shaller, P.J., 1991. Analysis of a large moist landslide, Lost River Range, Idaho, U.S.A. Canadian Geotechnical Journal = Revue Canadienne de Geotechnique 28 (4), 584–600.
Shea, T., van Wyk de Vries, B., Pilato, M., 2008. Emplacement mechanisms of contrasting debris avalanches at Volcán Mombacho (Nicaragua), provided by structural and facies analysis. Bulletin of Volcanology 70 (8), 899–921.
Siebe, C., Komorowski, J.C., Sheridan, M.F., 1992. Morphology and emplacement of an unusual debris-avalanche deposit at Jocotitlán Volcano, Central Mexico. Bulletin of Volcanology 54 (7), 573–589.
Siebert, L., 1984. Large volcanic debris avalanches: characteristics of source areas, deposits, and associated eruptions. Journal of Volcanology & Geothermal Research 22 (3–4), 163–197.
Siebert, L., 2002. Landslides resulting from structural failure of volcanoes. Reviews in Engineering Geology 15, 209–235.
Siebert, L., Beget, J.E., Glicken, H., 1995. The 1883 and late-Prehistoric eruptions of Augustine Volcano, Alaska. Journal of Volcanology & Geothermal Research 66 (1–4), 367–395.
Smith, G.M., Davies, T.R., McSaveney, M.J., Bell, D.H., 2006. The Acheron rock avalanche, Canterbury, New Zealand: Morphology and Dynamics. Landslides 3 (1), 62–72.
Sparks, R.S.J., Gardeweg, M.C., Calder, E.S., Matthews, S.J., 1997. Erosion by pyroclastic flows on Lascar volcano, Chile. Bulletin of Volcanology 58 (7), 557–565.
Van Wyk De Vries, B., Self, S., Francis, P.W., Keszthelyi, L., 2001. A gravitational spreading origin for the Socompa debris avalanche. Journal of Volcanology and Geothermal Research 105 (3), 225–247.
von Poschinger, A., 1994. Some special aspects of the “impact” of a landslide on the valley floor. Landslide News 8, 26–28.
von Poschinger, A., Wassmer, P., Maisch, M., 2006. The Flims rockslide; history of interpretation and new insights. In: Evans, S.G., Scarascia-Mugnozza, G., Strom, A.L., Hermanns, R.L. (Eds.), Landslides from Massive Rock Slope Failure. Nato Science Series IV, Earth and Environmental Sciences, Vol.49, pp. 329–356.
Wright, C.A., 1998. The Ad 930 long-runout Round Top debris avalanche, Westland, New Zealand. New Zealand Journal of Geology and Geophysics 41 (4), 493–497.
Yarnold, J.C., Lombard, J.P., 1989. Facies model for large rock avalanche deposits formed in dry climates. In: Colburn, I.P., Abbott, P.L., Minch, J. (Eds.), Field Trip Guidebook — Pacific Section, Society of Economic Paleontologists and Mineralogists, Vol. 62, pp. 9–31.